Article

Automatic Extension of a Semi-Detailed Synthetic Fuel Reaction Mechanism

Marleen Schmidt *, Celina Anne Kathrin Eberl, Sascha Jacobs, Torsten Methling [ID], Andreas Huber and Markus Köhler [ID]

German Aerospace Center (DLR), Institute of Combustion Technology, 70569 Stuttgart, Germany;
celinaeberl@gmx.de (C.A.K.E.); sascha.jacobs@dlr.de (S.J.); torsten.methling@dlr.de (T.M.);
andreas.huber@dlr.de (A.H.); m.koehler@dlr.de (M.K.)
* Correspondence: marleen.schmidt@dlr.de; Tel.: +49-711-686-285-63

Abstract: To identify promising sustainable fuels, e.g., to select novel synthetic fuels with the greatest impact on minimizing global warming, new methods for rapid and economical technical fuel assessment are urgently needed. Here, numerical models that are capable of predicting technical key data quickly and without experimental setup are necessary. One method is the use of chemical kinetic models, which are able to predict the technical key parameters related to combustion behavior. For a rapid technical fuel assessment, these chemical kinetic models need to be validated for new fuel components and for different temperature and pressure ranges. This work presents a new approach to extend the existing semi-detailed chemical kinetic models. For the application of the approach, the semi-detailed reaction mechanism DLR Concise was selected and extended for the low temperature combustion modeling of n-heptane and isooctane. The open-source software reaction mechanism generator (RMG) was used for this extension. Furthermore, an optimization of the merged chemical kinetic model with the linear transformation model (linTM) was conducted in order to improve the reproducibility of ignition delay times. The improvement of the predictive performance of ignition delay times at low temperatures for both species was successfully demonstrated. Therefore, this approach can be used to quickly add new species or reaction pathways to an existing semi-detailed reaction mechanism to enable a model-based technical fuel assessment for the early identification of promising fuels.

Keywords: chemical kinetic mechanism; automatic model generation; synthetic fuels; model optimization; RMG; semi-detailed; surrogate mechanism

1. Introduction

Sustainable fuels produced from renewable resources are necessary to replace fossil aviation and transportation fuels [1,2] and to address a sustainable mobility, thus mitigating climate effects [3]. Questions of production, composition, and potential are currently investigated with high intensity [3,4]. The path for novel candidates prior to application is regulated by certification processes due to reasons of safety and compatibility, like ASTM D4054 [5] for aviation fuels, and ASTM D975 [6] for diesel fuels. Technical key parameters like the research octane number (RON) for gasoline or the derived cetane number (DCN) for promising diesel and sustainable aviation fuels (SAF) candidates need to be predicted within the certification process. In addition, the lean blowout (LBO) needs to be determined as it represents a safety criteria in the aviation sector.

These certification processes are costly and time-consuming, e.g., due to extensive experimental testing [7]. To accelerate the certification process and to decrease the costs, numerical methods are developed to reduce the experimental efforts, or even to fully replace the experimental prediction of technical key parameters. These technical key parameters are estimated via physical models, simulation, regression, or artificial intelligence

approaches [8,9]. The cetane number and the lean blowout are both dependent on physical processes, such as evaporation, and chemical processes, like autoignition [4,10,11].

The autoignition process can be effectively modeled using chemical kinetic models. Badra et al. [12] used a chemical kinetic model to predict the ignition delay time in order to deviate a technical key parameter. Fioroni et al. [13] and Westbrook et al. [14] also used reaction mechanisms to model the RON. Zhang et al. [15] used a chemical kinetic model for the prediction of the anti-knock tendency of gasoline additives. Schlichting et al. [16] developed a tool for predicting the RON based on chemical kinetic models. Schmidt et al. [8] used a chemical kinetic model for predicting the ignition delay time, and then utilized this ignition delay time alongisde physical fuel properties to predict the DCN.

These chemical kinetic models are developed for specific species of interest, and validated with fundamental experimental data, such as ignition delay times, laminar burning velocities, and species profiles measured in chemical reactors and reactive laminar flows. Thereby, the quality of the predictive capability of chemical kinetic reaction mechanisms is of the utmost importance for the adequate numerical evaluation of technical fuels [8,16].

Novel technical fuels consist of complex chemistry, involving many components in varying compositions [17]. To allow the chemical kinetic combustion modeling of novel fuels and their components, new reaction mechanisms need to be developed, or rather existing ones need to be extended. This requires the flexible addition of numerous new species and reaction pathways into reaction mechanisms. In order to cope with the complexity of these species and reaction additions, different automatized numerical approaches have been developed. Examples of currently actively developing projects are the reaction mechanism generator (RMG) [18,19], Auto-Mech [20], Chemtrayzer [21], and Genysis [22]. The RMG (version 3.10) is an opensource-based software, which integrates well with the Python environment and Cantera. The software has been extensively used [23], demonstrating its broad applicability.

The reaction mechanism generator (RMG) is a powerful software tool used in chemical kinetics to predict and analyze reaction mechanisms. The RMG is an automatic chemical reaction mechanism generator that constructs kinetic models comprised of elementary chemical reaction steps. This is achieved through general understanding of chemical processes and the exploration of complex reaction networks. Contemporarily, the RMG is the most-used software for generating reaction mechanisms [22]. The RMG automatically extends the reaction pathways and the thermochemistry (heat capacity, enthalpy, and entropy) for a given fuel at a given temperature and pressure range. Utilizing this software to generate reaction mechanisms can lead to models with high numbers of species and reactions. Zhang et al. [15] developed a reaction mechanism via the RMG for gasoline additives. Their detailed model featured 1456 species and 27,428 reactions. Liu et al. [24] modeled the acetylene pyrolysis and generated the reaction mechanism with the RMG. Their reaction mechanism had 1594 species and 8924 reactions. Dana et al. [25] developed a model via the RMG to describe the pyrolysis and oxidation of nitrogenous species ethylamine with 79 species and 1771 reactions. Nadiri et al. [26] used the RMG to generate a detailed chemical kinetic reaction mechanism for ammonia/methanol blends, which consist of thousands of reactions. In a postprocessing step, they reduced the number of species and reactions in the RMG-generated model for the feasible application of the model in numerical tools, such as computational fluid dynamics (CFD).

Various methods exist to reduce the number of species and reactions in chemical kinetic models, for instance, the lumping of species and reactions [23]. Exemplarily, the DLR Concise reaction mechanism [27] is designed as a semi-detailed compact chemical kinetic mechanism, combining detailed and lumped species and reactions. This reaction mechanism is validated against a broad range of experiments and is able to predict the combustion behavior of real fuels, represented by surrogate fuels. It is only developed for high temperature (HT) combustion regimes, focusing on the relevant combustion, e.g., for gas turbine conditions.

This approach presents a new numerical tool for rapidly extending an existing semi-detailed chemical kinetic reaction mechanism to new temperatures, pressure ranges, and fuel components. To demonstrate the new approach, the DLR Concise from Kathrotia et al. [27] is extended to allow the modeling of low-temperature chemical kinetics for the fuel species n-heptane and isooctane, specifically focusing on ignition delay times. As a pre-processing step, the DLR Concise is reduced to the core chemistry, and this is used as an Input for the RMG. The main approach deals with the processing of the resulting mechanism. As a last step, both the developed reactions for n-heptane and isooctane are merged together. The new approach demonstrates rapid model extensions, facilitating efficient chemical kinetic-supported technical fuel assessments and CFD simulations.

2. Materials and Methods

The DLR Concise is currently able to describe high temperature chemistry. The objective of the mechanism extension is the implementation of reaction steps that allow for the accurate modeling of ignition delay times at low temperature chemistry regimes. Figure 1 gives a short overview about the main reaction pathways or reaction families, which occur at both high and low temperatures. Low-temperature (LT) chemistry encompasses species with a peroxide group $R\dot{O}_2$, an hydroperoxide group $\dot{Q}OOH$, and species with both peroxide and hydroperoxide groups $\dot{O}OQOOH$ [28]. The corresponding decomposition reaction pathways are determined using RMG software. To extend the DLR Concise reaction mechanism with the new low-temperature reaction pathways for both n-heptane and isooctane, the approach of this study is divided into three parts and is explained in detail.
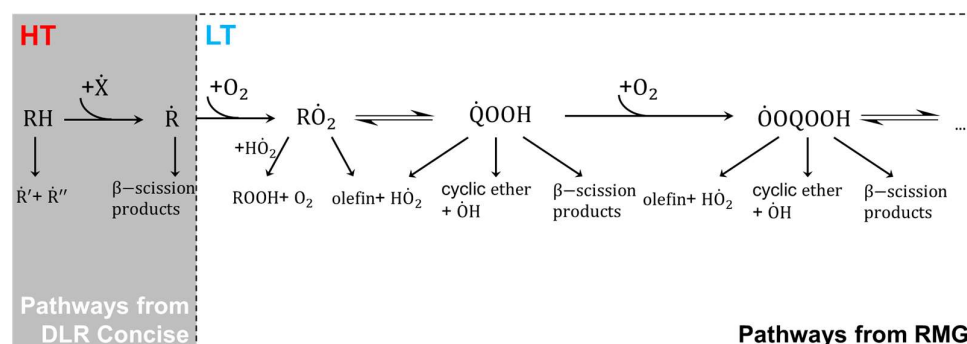

Figure 1. Scheme of a fuel oxidation based on work by Curran et al. [29], with $\dot{X}$ as $\dot{O}H$, $H\dot{O}_2$, $CH_3\dot{O}_2$, $\dot{H}$, $\dot{C}H_3$ radicals, and O-atoms as reactive species.

Figure 2 describes the extension of the low-temperature chemistry of a semi-lumped reaction mechanism for a fuel. The approach is divided into pre-processing, the main approach, and post-processing.

The pre-processing sets the boundary condition for the RMG. The boundary conditions are selected to cover the pressure, temperature, and composition regimes of the experiments of interest. In the following, only the ignition delay times measured in a shock tube are considered as experimental targets. Uncertainties in the generated mechanisms come from estimating the rate constants and thermochemistry, as well from using experimental data for the validation [30]. The uncertainties from rate rules are smaller than the ones from the species' thermochemistry. Due to the lack of sparse information on the uncertainties of rate rules, no further conclusion can be made [31].

The main approach deals with the intermediate results, including model analyses and adaptations. The combination of each individual *optimized* model into a final model, also known as the automated surrogate mechanism (AutoSM), occurs during post-processing. The entire approach needs to be executed for every fuel component of interest when modeling its low-temperature chemistry pathways. Every reaction mechanism is validated with the simulation of a zero-dimensional, constant enthalpy and pressure reactor in the open-source software Cantera (version 2.5.1) [32]. For every initial temperature, pressure,

and composition of interest, a reactor is simulated. The time of the maximum temperature rise is used as the ignition delay time. The results were compared with the experimental data of the single fuel component measured in a shock tube.
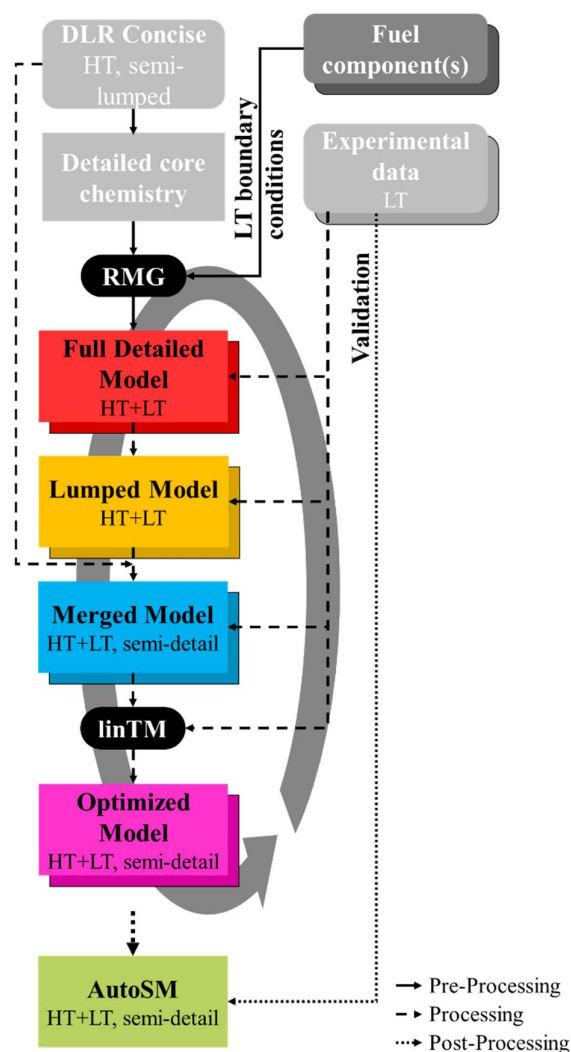
Figure 2. Scheme of the extension of a semi-lumped reaction mechanism for the LT regime of a fuel, using the opensource software RMG [18,19] and the linTM approach [33].

2.1. Pre-Processing

The reaction mechanism of DLR Concise [27] needs to be condensed to focus on the core chemistry, which includes the reactions involving C0-C4 species. Additionally, it should be translated into a non-lumped version, detailing the core chemistry. This reaction mechanism is used as the input for the RMG [18,19]. Beside the detail core chemistry, the Klippenstein–Glarborg reaction mechanism and the Glarborg-C3 reaction mechanism, both already implemented by the RMG, were chosen as additional input libraries. All reaction mechanisms are clustered under reactionLibraries (see Table 1). For the thermochemistry libraries (thermoLibraries), the data from the corresponding reactionLibraries are selected: the detail core chemistry, the Klippenstein–Glarborg, and the primaryThermoLibrary from the RMG. As an input, different reactor types for gaseous systems or for liquid systems can be chosen [19]. Reactor setups can be arranged to cover ranges of different initial temperatures, pressures, and compositions [19]. Additional ranged reactors can be used by defining a range of initial conditions [19].

Table 1. RMG settings for n-heptane and isooctane.

	n-Heptane	Isooctane
thermoLibraries	'Detailed_core_chemistry' 'Klippenstein_Glarborg2016' 'primaryThermoLibrary'	
reactionLibraries	'Detailed_core_chemistry' 'Klippenstein_Glarborg2016' 'Glarborg/C3'	
Temperature in K	650–1200	600–1200
Pressure in bar	1–20	20–55
Equivalence ratio Φ	1	
nSims	12	
terminationConversion	0.9	
terminationTime in s toleranceKeepInEdge	20 0.01	
toleranceMoveToCore	0.1	
toleranceBranchReactionToCore	0.001	-
branchingIndex	0.5	-
branchingRatioMax	1	-
toleranceInterruptSimulation	10^8	
maximumEdgeSpecies	10^5	
filterReactions	True	

To select a sample from the range of the initial conditions, the RMG utilizes an algorithmic based on a weighted stochastic grid. This algorithm also incorporates the conditions of the previous runs of the process. Every sample needs to run successfully multiple times (nSims). According to the RMG guidelines, nSims was fixed to 12 [18,19]. During the run, the RMG identifies important species using a rate-based algorithm. If the flux of a species is higher than the parameter toleranceMoveToCore, the species is added to the core model [18,19,29]. Other species which might be important but are under the value of toleranceMoveToCore and above the value of toleranceKeepInEdge are added into an edge model. Species with a flux lower than toleranceKeepInEdge are no longer considered in that run. If a species has an equal or higher flux than the parameter toleranceInterruptSimulation, the run is stopped, due to the unrealistic value, which occurs in incomplete mechanisms. The maximum number of edge species is limited to 10^5 due to memory constraints. This limitation can affect the full detailed model (see Figure 2). To speed up the RMG run and the pre-filtering reactions, as is recommended by the software, the value of filterReactions was set to True. The values for model parameters were chosen, according to the RMG guidelines. The RMG develops reaction rates based on the estimation of kinetics. Before calculating the reaction rates, the RMG checks if the rates of the desired reaction are already implemented in any reactionLibraries. Afterwards, the reaction rates are estimated based on reaction families. An automatically generated decision tree is used to identify the proper reaction family. Each reaction family has reaction rules and rates defined in reaction templates. Depending on the reaction families and the reactants involved in the reaction, the decision tree algorithm selects the appropriate reaction template. Currently, 74 reaction families are defined in the RMG [19]. The thermodynamic properties for the developed RMG species are taken from the thermoLibraries, or in cases where they do not exist, added by the RMG, which estimates them according to the group contribution methods [19].

The reactor settings of the RMG were set with a ranged reactor with a variation of temperature T and pressure p, whereas the fuel–air equivalence ratio ϕ is fixed to

a stoichiometric combustion (see Table 1). The settings were determined based on the experimental data for n-heptane and isooctane from Shao et al. [34].

Using an advanced model setting, according to the RMG guidelines for species with a distinct NTC (negative temperature coefficient) behavior, like *n*-heptane, can provide an improved model. By using this branching criterion, species that have a low flux, but are essential for branching reactions are also considered [18,19,35]. In particular, species like the hydroperoxyl radical ($H\dot{O}_2$), the hydroxide ($\dot{O}H$), or a hydrocarbon radical ($\dot{R}$) and their products (see Figure 1) are very important at low temperatures [28]. The settings are chosen according the RMG guideline.

To guarantee that the fuel is consumed and to reduce the computational effort, two termination conditions were defined. First, the modelling time of the reactor was limited to the time when 90% of the reactant was consumed (terminationConversion). Second, the time when the reactor is terminated was set to 20 s (terminationTime).

For the practical implementation and generation of a reaction mechanism, an investigation of each iterative model was conducted (see Figure S1). In order to monitor and evaluate the state of the predictive capability of the model, the sum of logarithmic differences d_{sum} between the experimental and simulated ignition delay times was selected as an evaluation value, as shown in Equation (1):

$$d_{sum} = \frac{1}{n}\sum_{j=0}^{n} |d_j| = \frac{1}{n}\sum_{j=0}^{n}\left| \ln\left(\frac{\tau_{ign}^{exp}(T_j)}{\tau_{ign}^{sim}(T_j)} \right) \right| \qquad (1)$$

where n is defined as the amount of the experimental data, d_j as the logarithmic difference between experiment and simulation, τ_{ign} as the ignition delay time, T as the temperature, and the superscripts *exp* and *sim* are indicating experimental and simulation data, respectively. If the logarithmic sum of deviations d_{sum} does not change significantly, it was assumed that sufficient species and reactions were added during the mechanism generation process, and the mechanism was completed. Hence, the generation process could be terminated earlier in order to save computational time [36]. If the d_{sum} stayed constant, the run was stopped and the first iterative model that met the above conditions was selected. Here, the extended detailed reaction mechanism of the detailed core chemistry of the DLR Concise is referred to in the *full detailed* model (see Figure 2 (red block)).

2.2. Processing

The *full detailed* model consists of the DLR Concise core detailed model, as well as new species and reactions added by the RMG. Different isomers are lumped together in the original DLR Concise model. To facilitate the subsequent merging step, the same isomers must be lumped into the *full detailed* model. The lumping of isomers can lead to duplicate reactions. For these reactions, rate coefficients were defined as the sum of the rate coefficients of all duplicate reactions.

The *lumped* model is then merged to the DLR Concise to create the *merged* model (see Figure 2 (blue box)). Some reactions are present in both the *lumped* model and DLR Concise. For these reactions, only the DLR Concise reactions were kept, and only new reactions from the *lumped* model were added (see Figure S2). Since the DLR Concise was developed and validated for HT application, there might be some reaction parameters which are not suitable for LT application. These reactions can lead to significant changes in the predictive capability between the *lumped* and the *merged* model.

To identify these reactions, the DLR Concise reactions were replaced one after the other with the corresponding reaction from the *lumped* model. The ignition delay time at the temperature of interest was analyzed for every changed reaction. In cases of significant shifts and for low temperature reaction pathways (see Figure 1) the DLR Concise reaction was updated with the reaction proposed by RMG, stemming from the reactionLibraries or rate rule approaches. The thermodynamic data of additional species were merged with the DLR Concise thermodynamic data. In addition, an analysis was conducted to identify

the differences between the thermodynamic properties of the DLR Concise and the *lumped* model. In cases in which changes of thermodynamic data from the RMG had a significant impact on the predictive capability the DLR Concise, the species properties were updated.

Adapting the DLR Concise reactions and, if necessary, the thermodynamic properties in the *merged* model results in the adapted *merged* model. The adapted merged model underwent optimization against experimental ignition delay times using the linear transformation model (linTM) [33], which has demonstrated high efficiency, effectiveness, and robustness in optimizing chemical kinetics [33,37]. The linTM optimizes the reaction rate coefficients to reduce the deviations between the modeled data and the quantities of interest, like ignition delay times, laminar burning velocities, or species profiles in chemical reactors or reactive laminar flows [37]. As a peculiarity, the linTM approach does not directly optimize the Arrhenius coefficients of the reaction rate k due to the dependence of the domain boundaries on the values of the individual Arrhenius parameter [33]. In order to obtain independent domain boundaries, the optimization parameters are logarithmic differences $\Delta \ln k$ to the base value of k at three user-defined temperatures T_i [33]. All optimized parameters are normalized with their maximum value in order to form the optimization or input parameter τ_i. In this work, the quantities of interest are the ignition delay times of n-heptane and isooctane measured in a shock tube by Shao et al. [34]. The linTM defines the sensitivity $S_{r,j}$ of each reaction r on the distance d_j as the Euclidean sum of the squares of the weighted gradients:

$$S_{r,j} = \left(\sum_{i=m}^{m+P_r-1} \left(w_j \frac{\partial d_j}{\partial \tau_i} \right)^2 \right)^{0.5} \qquad (2)$$

where w_j is the weighting factor, P_r is the number of optimization parameters of reaction r, and m is a control variable. The global sensitivity of a reaction is defined as the sum of all sensitivities $S_{r,j}$ for all D distances.

The global sensitivity of a reaction S_r is estimated as follows:

$$S_r = \sum_{j=1}^{D} S_{r,j} \qquad (3)$$

All reactions that were added by the RMG to the original DLR Concise mechanism were investigated with the global sensitivity analysis on the ignition delay times, and the reaction rate of the most sensitive reactions were optimized. The logarithmic difference between the optimized and original values of the rate coefficients Δlnk must be less than a defined value. This means that the optimization was conducted within the local solution space of the rate coefficients $\Delta lnk(T_i) = 0.5$ [33]. The optimization or input parameters of the reactions were optimized within 3 σ, with the uncertainty of 2 σ set to $\Delta lnk(T_i) = 0.5$, which is a common assumption for estimated rate coefficients [38].

2.3. Post-Processing

In the last step (see Figure 2: green block), all *optimized* models for every fuel component were hierarchically combined into one single automated surrogate mechanism (AutoSM), and the predictive capability on the ignition delay times was analyzed. In detail, the optimized models of *n*-heptane and isooctane contain reactions that were present in both models. They also had reactions which are not present in the other model. By combing the two in AutoSM, the *n*-heptane model was used as the base model, and only new reactions and species from the isooctane model were added to the *n*-heptane model.

The predictive capability was compared with other reaction mechanisms [39,40]. Reaction mechanisms from Ranzi et al. [39] of the Polytechnic University of Milan (POLIMI) and Mehl et al. [40] of the Lawrence Livermore National Laboratory (LLNL) are detailed and validated for simulating technical or surrogate fuels. The predictions of the ignition delay times with the AutoSM, POLIMI, and LLNL mechanisms were compared via the

logarithmic differences d_{sum} of the experiment to the mechanism in order to evaluate the model performances.

3. Results and Discussion

As a proof of concept, the presented approach is applied to the DLR Concise [27] in order to extend the low-temperature combustion pathways of n-heptane and isooctane. For the overall validation of the AutoSM, the model performance is compared with the measured ignition delay times of different primary reference fuel (PRF) mixtures, containing n-heptane and isooctane.
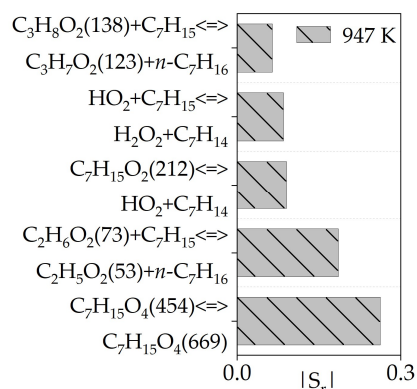
3.1. n-Heptane

Figure 3 compares the simulated ignition delay times of the original DLR Concise reaction mechanism [27] and the models of the main approach with the experimental ignition delay times of n-heptane in air at a pressure of 28 atm under stoichiometric conditions (ϕ = 1), as measured by Shao et al. [34] in a shock tube. For this condition, the original DLR Concise, developed for HT application, predicts the combustion characteristics in the HT regime. At LTs, the DLR Concise reaction mechanism is not capable of predicting the experimental data due to the lack of LT-chemistry pathways, whereas the *full detailed* model is capable of predicting the experimental data. The *full detailed* model is able to reproduce the NTC behavior.
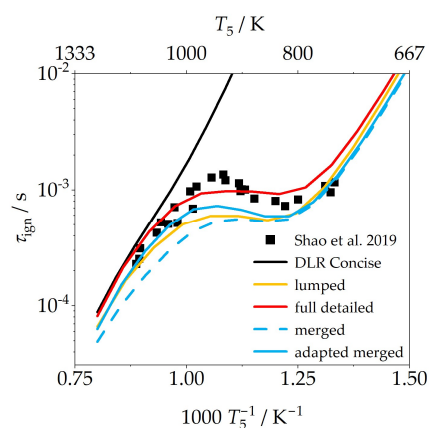
Figure 3. Simulation of the chemical ignition delay times τ_{ign} of n-heptane in air with ϕ = 1 at p = 28.4 bar in a shock tube with the experimental shock tube data from Shao et al. [34].

Like the *full detailed* model, the *lumped* model shows a distinct NTC behavior. Between the temperatures of 800 K and 1000 K, the *lumped* model underestimates the experimental ignition delay times. When compared to the *lumped* model, the *merged* model predicts precise ignition delay times at LTs, whereas the ignition delay time at HTs is overpredicted. To improve the predictive capability of the *merged* model, the *lumped* model reactions were successively replaced by the corresponding reaction from the DLR Concise (see Figure S3a). One reaction was identified and was replaced with the corresponding reactions, developed by the RMG (see Figure S3b and Table S1). The performance of the *adapted merged* model is presented in Figure 3. For a detailed description, see Supplementary Section S1.2.

To further improve the performance of the chemical kinetic model of n-heptane, further analysis was performed, and the optimization with the linTM [33] was conducted. A global sensitivity analysis, as presented above, was undertaken for the *adapted merged* model to identify the most sensitive reactions. Only two reactions were considered for optimization: (i) those generated from the RMG and (ii) those containing a species with a chain length of seven carbon atoms. Furthermore, the global sensitivity analysis for n-heptane was performed at a temperature of 947 K and a pressure of 28.4 bar under stoichiometric conditions (see Figure 4).

Figure 4. Sensitivity analysis of the *n*-heptane *adapted merged* model at $T = 947$ K and $p = 28.4$ bar under $\phi = 1$. $C_3H_8O_2(138)$: CCCOO; $C_3H_7O_2(123)$: CCCO[O]; $C_7H_{15}O_2(212)$: CCCCC(C)O[O]; $C_2H_6O_2(73)$: CCOO; $C_2H_5O_2(53)$: CCO[O]; $C_7H_{15}O_4(454)$: CCCC(CC(C)O[O])OO; $C_7H_{15}O_4(669)$: CCC[C](CC(C)OO)OO.

The most sensitive reactions presented in Figure 4 are the typical LT reactions, which are important for the decomposition of n-heptane. The two most sensitive reactions are optimized by using the linTM. The changed reaction rates are listed in the Supplementary Table S1. The performance of the *optimized* model of n-heptane is shown in Figure 5. The *optimized* model is able to precisely predict the ignition behavior at high and low temperatures. The optimization improved the predictive capability at temperatures between 800 K and 1000 K.
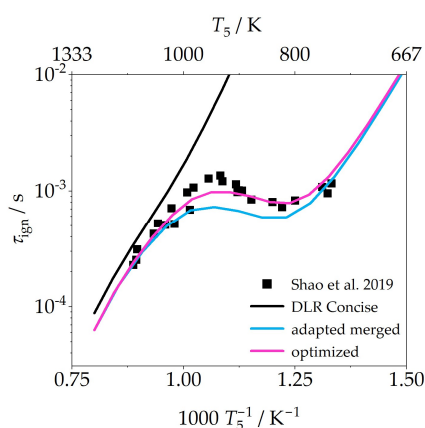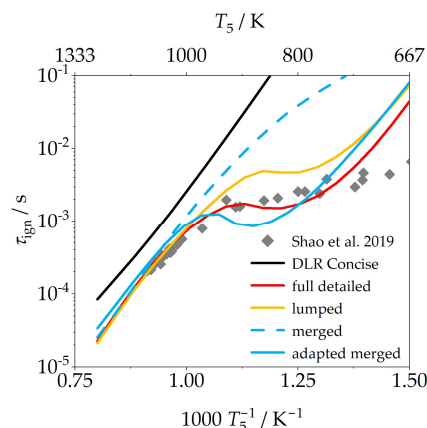

Figure 5. Simulation of the chemical ignition delay times τ_{ign} of n-heptane in air with $\phi = 1$ at 28.4 bar in a shock tube of the *optimized* and *adapted merged* model with the experimental shock tube data from Shao et al. [34].

3.2. Isooctane

Figure 6 shows the results of the extension of the DLR Concise reaction mechanism for isooctane. The DLR Concise is overestimating the experimental ignition delay times of isooctane. The *full detailed* model (see Figure 2, red block) accurately predicts the experimental data at HTs, but overpredicts the ignition delay times below 720 K. The *lumped* model overestimates the experimental data below 1000 K.

The *merged* model of the *lumped* model to the original DLR Concise significantly overestimates the ignition delay times below 1000 K (Figure 6). First, the thermodynamic properties of the DLR Concise were analyzed by investigating the influence of the corresponding thermodynamic properties of the species by the RMG on the *merged* model (see Figure S4a). In Figure S5, the entropy of the RMG isomers are compared to the DLR Concise and LLNL properties for isomers iC7H13 and iC7H14. The properties proposed by the RMG are the same as the ones defined by LLNL, whereas the DLR Concise predicts higher values for the entropy. Hence, these two thermodynamic properties of iC7H13 and iC7H14 were updated with the values from the RMG.

Figure 6. Simulation of the chemical ignition delay times τ_{ign} of isooctane in air with $\phi = 1$ at 55.7 bar in a shock tube with the experimental shock tube data from Shao et al. [34].

To further improve the predictive capability, the *lumped* model reactions were successively replaced by the corresponding reaction from the DLR Concise (see Figure S4b). One reaction was identified and was replaced with the corresponding reactions developed by the RMG (see Figure S6 and Table S3). For a detailed description, see Supplementary Section S1.3. As presented by Johnson et al., the RMG database is capable of predicting sufficiently accurate reaction rates and thermochemistry [18].

For isooctane, the same approach as for n-heptane is executed to improve the predictive capability of ignition delay times by optimization methods. First, the sensitivity of reactions was developed by the RMG, considering species consisting with a carbon length of 8 at a temperature of 918 K, a pressure of 55.7 bar, and $\phi = 1$, see Figure 7. At this temperature, only low-temperature reactions are sensitive to the ignition delay times. Hence, the two most sensitive reactions were optimized using the linTM. The optimized reactions rates are listed in Supplementary Table S3.
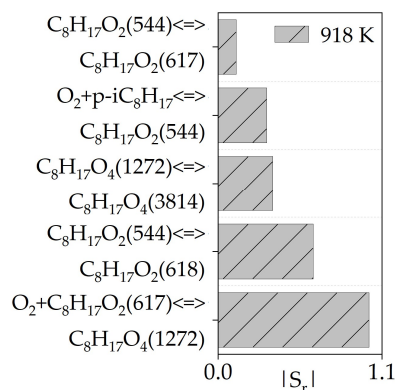
Figure 7. Sensitivity analysis of the *merged* model of isooctane at 918 K. $C_8H_{17}O_2(544)$: CC(C)CC(C)(C)CO[O]; $C_8H_{17}O_2(617)$: [CH2]C(C)(COO)CC(C)C; $C_8H_{17}O_4(1272)$: CC(C)CC(C)(CO[O])COO; $C_8H_{17}O_4(3814)$: CC(C)CC(C)([CH]OO)COO; $C_8H_{17}O_2(618)$: C[C](C)CC(C)(C)COO.

By adapting these two reactions with the optimization tool, the *optimized* model was conducted and compared to the adapted *merged* model; the performance was enhanced, as shown in Figure 8.
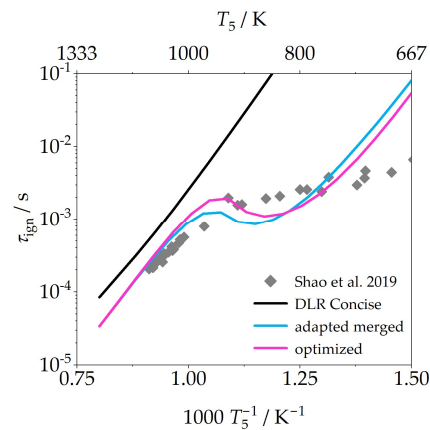
Figure 8. Simulation of the chemical ignition delay times τ_{ign} of isooctane in air with $\phi = 1$ at 55.7 bar in a shock tube of the *adapted merged* and *optimized* model with the experimental shock tube data from Shao et al. [34].

3.3. Overall Model Validation

Both optimized submodels for n-heptane and isooctane were added to the DLR Concise in order to form the automated surrogate mechanism (AutoSM) (see Figure 2). The performance of this AutoSM on the ignition delay times of n-heptane, isooctane, and their mixtures as a primary reference fuel (PRF) are compared to the performance of the two established models by Ranzi et al. [39] (POLIMI) and Mehl et al. [40] (LLNL) (see Figure 9). PRF60 is a volumetric mixture of 40 vol.% of n-heptane and 60 vol.% of isooctane. The experimental data of PRF60 and PRF70 are both measured in a shock tube at stoichiometric conditions. The experimental data of PRF60 are conducted at 40 bar, whereas the data of PRF70 are conducted at 20 bar.
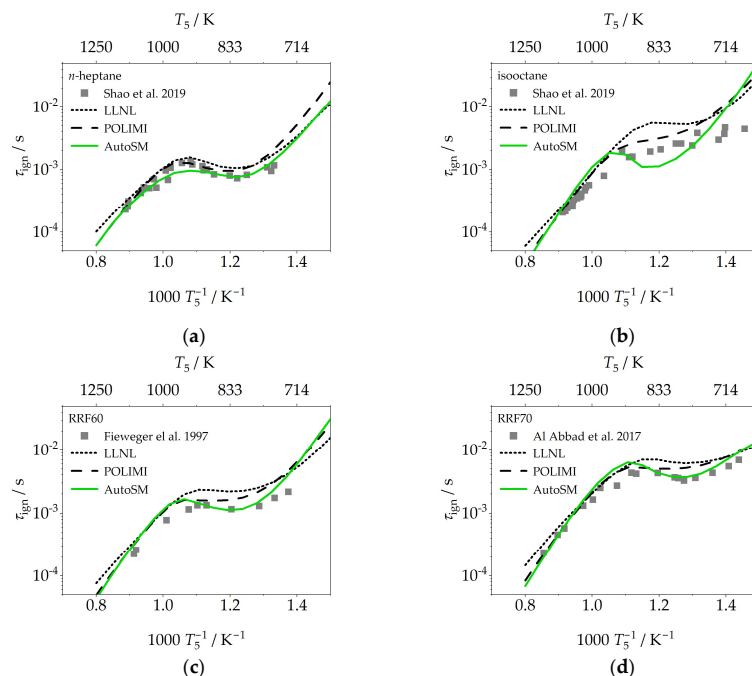
Figure 9. Simulation of the chemical ignition delay times τ_{ign} of (**a**) n-heptane at 28.4 bar; (**b**) isooctane at 55.7 bar; (**c**) PRF60 at 40 bar; (**d**) PRF70 at 20 bar in air with $\phi = 1$ in a shock tube of the AutoSM, the POLIMI [39], and LLNL [40] with the experimental shock tube data from Shao et al. [34], Fieweger et al. [41], and Al Abbad et al. [42].

All models show similar performances for n-heptane, see Figure 9a. For isooctane, see Figure 9b, the LLNL model overpredicts the combustion behavior, whereas the POLIMI slightly overpredicts, and the AutoSM slightly underpredicts the ignition delay times. The predictive capability of PRF60 and PRF70 depends on the performance of the pure components. Hence, the LLNL has been compared to the Polimi and the AutoSM, expressing slightly lower predictive capability, see Figure 9c,d.

For n-heptane, PRF60, and PRF70, the developed AutoSM shows the best performance when compared to the literature models (POLIMI, LLNL), resulting in a low d_{sum}. The POLIMI model has the smallest d_{sum} for isooctane, followed by the AutoSM. The LLNL, as seen already in Figure 9b, overpredicts isooctane ignition delay times, leading to a higher deviation between the experimental and the simulated ignition delay times. With higher isooctane contents, the deviations of the LLNL increase (see PRF70 in Table 2).

Table 2. d_{sum} of the corresponding experiment, and the prediction of the used mechanism, according to Equation (1).

Mechanism	*n*-Heptane	Isooctane	PRF60	PRF70
POLIMI	5.09	12.63	3.94	4.40
LLNL	7.01	16.33	5.56	6.43
AutoSM	3.50	14.38	1.65	2.44

In summary, the AutoSM is capable of describing the ignition delay time, similarly to the established POLIMI mechanism, and also has a superior performance than the LLNL mechanism.

To test the AutoSM, the oxidation of *n*-heptane was further investigated by simulating a jet-stirred reactor at 1.06 bar, a residence time of 2 s, and ϕ = 0.9 diluted in helium [43]. Figure S7 shows the results of predicting the mole fractions of *n*-heptane and oxygen. For both species, the experimental data are reproduced at HT above 800 K. Below 700 K, the mole fraction of oxygen is described accurately, whereas the decomposition of n-heptane in the LT region is slightly overestimated.

To demonstrate the applicability of the AutoSM in predicting technical key parameters, the approach from Schmidt et al. [8] was used to estimate the DCN of PRF. The ignition delay times of *n*-heptane, isooctane, and PRF10-95 were simulated with the model AutoSM and used in Equations (S1)–(S3). The results are in a ±5 range (see Figure S8). The use of AutoSM with a focus on the ignition delay of the playback presents an accurate prediction of DCN.

4. Conclusions

This work presents a novel approach for the partially automatic extension of a semi-detailed reaction mechanism. An existing mechanism can be extended for new species (submodels), including the extension of variable-validated boundary conditions, like low-temperature combustion chemistry. With the developed approach, consisting of pre-processing, the main approach, and post-processing, an automatically developed surrogate mechanism (AutoSM) was developed. For the pre-processing, the reaction mechanism generator (RMG) software was used to get a detailed reaction mechanism. With the main approach, a new method was established for merging the original mechanism with the detailed mechanism produced by the RMG. A semi-automatic investigation was conducted for the adaptation of the merged mechanism. For the next step, the linTM [33] was used to optimize the *merged* model. Finally, all submodels were merged together to make the automated surrogate mechanism (AutoSM). As a proof of concept, the semi-detailed HT model (DLR Concise) was extended with the required reaction pathways for the low-temperature combustion modeling of n-heptane and isooctane. The results of this investigation have shown that the developed AutoSM presents a satisfying performance in predicting ignition delay times when compared to the POLIMI and demonstrates an improved performance when compared to the LLNL model for the pure components, as well as for PRF60 and PRF70.

The presented approach can be used for a rapid extension of numerically efficient semi-detailed chemical kinetic models. New surrogate mechanisms can be developed quickly for predicting the combustion behavior of novel fuels. This method can support fast technical fuel assessments in order to access the need for reaction mechanisms, validated for surrogate components and temperature and pressure regimes.

Supplementary Materials: The following supporting information can be downloaded at: https://www.mdpi.com/article/10.3390/en17050999/s1, Figure S1. Simulation logic of identifying the *extended* mechanism; Figure S2. Simulation logic of *merging* the *lumped* model to the DLR Concise reaction mechanism; Table S1. *N*-heptane reactions rates of the DLR Concise and *lumped* model; Figure S3. (a) Cumulative replacement of the reactions data and investigation. Simulation of the chemical ignition delay time τ_{ign} of *n*-heptane in air at 1100 K with $\phi = 1$ at 28.4 bar. (b) Reaction rate of identified reaction of (a) the *adapted lumped* model compared to the DLR Concise, LLNL and Polimi reaction mechanism; Table S2. *N*-heptane reactions rates of the *merged* and *optimized* model. Figure S4. Simulation of the chemical ignition delay time τ_{ign} of isooctane in air at 833 K with $\phi = 1$ at 55.7 bar. (a) Comparison of the influence of the thermochemistry of each species. (b) Cumulative replacement of the reactions data and investigation; Figure S5. Entropy of the species iC7H13 and iC7H14 from the DLR Concise compared to the entropy properties of the isomers of iC7H13 and iC7H14 of the *extended* model and the LLNL; Table S3. Isooctane reactions rates of the DLR Concise and the *adapted lumped* model; Figure S6. Reaction rate of the *adapted lumped* model compared to the DLR Concise, LLNL and Polimi reaction mechanism; Table S4. Isooctane reactions rates of the *merged* and *optimized* model; Figure S7. Simulation a jet-stirred reactor of *n*-heptane at 1.06 bar, a residence time of 2 s and $\phi = 0.9$ diluted in helium [29]; Figure S8. Using the approach from Schmidt et al. [8] and demonstrating the potential of the AutoSM for predicting technical key parameters like the DCN.

Author Contributions: Conceptualization: M.S. and T.M.; methodology: M.S.; validation of software approach: M.S. and C.A.K.E.; investigation, M.S., S.J. and T.M.; writing—Original Draft Preparation: M.S.; writing—review and editing, M.S., S.J., T.M., A.H. and M.K.; supervision, A.H. and M.K. All authors have read and agreed to the published version of the manuscript.

Data Availability Statement: The data presented in this study are available on request from the corresponding author.

Conflicts of Interest: The authors declare no conflicts of interest.

References

1. Wang, M.; Dewil, R.; Maniatis, K.; Wheeldon, J.; Tan, T.; Baeyens, J.; Fang, Y. Biomass-derived aviation fuels: Challenges and perspective. *Prog. Energy Combust. Sci.* **2019**, *74*, 31–49. [CrossRef]
2. Drünert, S.; Neuling, U.; Zitscher, T.; Kaltschmitt, M. Power-to-Liquid fuels for aviation—Processes, resources and supply potential under German conditions. *Appl. Energy* **2020**, *277*, 115578. [CrossRef]
3. Kohse-Höinghaus, K. Combustion in the future: The importance of chemistry. *Proc. Combust. Inst.* **2020**, *38*, 1–56. [CrossRef] [PubMed]
4. Heyne, J.; Rauch, B.; Le Clercq, P.; Colket, M. Sustainable aviation fuel prescreening tools and procedures. *Fuel* **2021**, *290*, 120004. [CrossRef]
5. D02 Committee. *Practice for Evaluation of New Aviation Turbine Fuels and Fuel Additives*; ASTM International: West Conshohocken, PA, USA, 2021.
6. D02 Committee. *Specification for Diesel Fuel*; ASTM International: West Conshohocken, PA, USA, 2022.
7. Rumizen, M.A. Qualification of Alternative Jet Fuels. *Front. Energy Res.* **2021**, *9*, 760713. [CrossRef]
8. Schmidt, M.; Schlichting, S.; Melder, J.; Methling, T.; Köhler, M.; Huber, A. Determination of Cetane Numbers via Chemical Kinetic Mechanism. *J. Eng. Gas Turbines Power* **2024**, *146*, 021018. [CrossRef]
9. Abdul Jameel, A.G.; van Oudenhoven, V.C.; Naser, N.; Emwas, A.-H.; Gao, X.; Sarathy, S.M. Predicting Ignition Quality of Oxygenated Fuels Using Artificial Neural Networks. *SAE Int. J. Fuels Lubr.* **2021**, *14*, 57–86. [CrossRef]
10. Peiffer, E.E.; Heyne, J.S.; Colket, M. Sustainable Aviation Fuels Approval Streamlining: Auxiliary Power Unit Lean Blowout Testing. *AIAA J.* **2019**, *57*, 4854–4862. [CrossRef]
11. Won, S.H.; Rock, N.; Lim, S.J.; Nates, S.; Carpenter, D.; Emerson, B.; Lieuwen, T.; Edwards, T.; Dryer, F.L. Preferential vaporization impacts on lean blow-out of liquid fueled combustors. *Combust. Flame* **2019**, *205*, 295–304. [CrossRef]

12. Badra, J.A.; Bokhumseen, N.; Mulla, N.; Sarathy, S.M.; Farooq, A.; Kalghatgi, G.; Gaillard, P. A methodology to relate octane numbers of binary and ternary n-heptane, iso-octane and toluene mixtures with simulated ignition delay times. *Fuel* **2015**, *160*, 458–469. [CrossRef]

13. Fioroni, G.M.; Rahimi, M.J.; Westbrook, C.K.; Wagnon, S.W.; Pitz, W.J.; Kim, S.; McCormick, R.L. Chemical kinetic basis of synergistic blending for research octane number. *Fuel* **2022**, *307*, 121865. [CrossRef]

14. Westbrook, C.K.; Sjöberg, M.; Cernansky, N.P. A new chemical kinetic method of determining RON and MON values for single component and multicomponent mixtures of engine fuels. *Combust. Flame* **2018**, *195*, 50–62. [CrossRef]

15. Zhang, P.; Yee, N.W.; Filip, S.V.; Hetrick, C.E.; Yang, B.; Green, W.H. Modeling study of the anti-knock tendency of substituted phenols as additives: An application of the reaction mechanism generator (RMG). *Phys. Chem. Chem. Phys.* **2018**, *20*, 10637–10649. [CrossRef]

16. Schlichting, S.; Methling, T.; Oßwald, P.; Zinsmeister, J.; Riedel, U.; Köhler, M. Numerical prediction of research octane numbers via a quasi-dimensional two-zone cylinder model. *Appl. Energy Combust. Sci.* **2022**, *11*, 100079. [CrossRef]

17. Melder, J.; Zinsmeister, J.; Grein, T.; Jürgens, S.; Köhler, M.; Oßwald, P. Comprehensive Two-Dimensional Gas Chromatography: A Universal Method for Composition-Based Prediction of Emission Characteristics of Complex Fuels. *Energy Fuels* **2023**, *37*, 4580–4595. [CrossRef]

18. Johnson, M.S.; Dong, X.; Grinberg Dana, A.; Chung, Y.; Farina, D.; Gillis, R.J.; Liu, M.; Yee, N.W.; Blondal, K.; Mazeau, E.; et al. RMG Database for Chemical Property Prediction. *J. Chem. Inf. Model.* **2022**, *62*, 4906–4915. [CrossRef] [PubMed]

19. Liu, M.; Grinberg Dana, A.; Johnson, M.S.; Goldman, M.J.; Jocher, A.; Payne, A.M.; Grambow, C.A.; Han, K.; Yee, N.W.; Mazeau, E.J.; et al. Reaction Mechanism Generator v3.0: Advances in Automatic Mechanism Generation. *J. Chem. Inf. Model.* **2021**, *61*, 2686–2696. [CrossRef] [PubMed]

20. Elliott, S.N.; Moore, K.B.; Copan, A.V.; Keçeli, M.; Cavallotti, C.; Georgievskii, Y.; Schaefer, H.F.; Klippenstein, S.J. Automated theoretical chemical kinetics: Predicting the kinetics for the initial stages of pyrolysis. *Proc. Combust. Inst.* **2021**, *38*, 375–384. [CrossRef]

21. Döntgen, M.; Przybylski-Freund, M.-D.; Kröger, L.C.; Kopp, W.A.; Ismail, A.E.; Leonhard, K. Automated discovery of reaction pathways, rate constants, and transition states using reactive molecular dynamics simulations. *J. Chem. Theory Comput.* **2015**, *11*, 2517–2524. [CrossRef] [PubMed]

22. Vandewiele, N.M.; van Geem, K.M.; Reyniers, M.-F.; Marin, G.B. Genesys: Kinetic model construction using chemo-informatics. *Chem. Eng. J.* **2012**, *207–208*, 526–538. [CrossRef]

23. Cavallotti, C. Automation of chemical kinetics: Status and challenges. *Proc. Combust. Inst.* **2023**, *39*, 11–28. [CrossRef]

24. Liu, M.; Chu, T.-C.; Jocher, A.; Smith, M.C.; Lengyel, I.; Green, W.H. Predicting polycyclic aromatic hydrocarbon formation with an automatically generated mechanism for acetylene pyrolysis. *Int. J. Chem. Kinet.* **2021**, *53*, 27–42. [CrossRef]

25. Dana, A.G.; Buesser, B.; Merchant, S.S.; Green, W.H. Automated Reaction Mechanism Generation Including Nitrogen as a Heteroatom. *Int. J. Chem. Kinet.* **2018**, *50*, 243–258. [CrossRef]

26. Nadiri, S.; Shu, B.; Goldsmith, C.F.; Fernandes, R. Development of comprehensive kinetic models of ammonia/methanol ignition using Reaction Mechanism Generator (RMG). *Combust. Flame* **2023**, *251*, 112710. [CrossRef]

27. Kathrotia, T.; Oßwald, P.; Naumann, C.; Richter, S.; Köhler, M. Combustion kinetics of alternative jet fuels, Part-II: Reaction model for fuel surrogate. *Fuel* **2021**, *302*, 120736. [CrossRef]

28. Warnatz, J.; Maas, U.; Dibble, R.W. *Combustion: Physical and Chemical Fundamentals, Modeling and Simulation, Experiments, Pollutant Formation*, 4th ed.; Springer: Berlin/Heidelberg, Germany, 2006; ISBN 3540259929.

29. Curran, H.J. Developing detailed chemical kinetic mechanisms for fuel combustion. *Proc. Combust. Inst.* **2019**, *37*, 57–81. [CrossRef]

30. Gao, C.W.; Liu, M.; Green, W.H. Uncertainty analysis of correlated parameters in automated reaction mechanism generation. *Int. J. Chem. Kinet.* **2020**, *52*, 266–282. [CrossRef]

31. Cai, L.; Pitsch, H. Mechanism optimization based on reaction rate rules. *Combust. Flame* **2014**, *161*, 405–415. [CrossRef]

32. Goodwin, D.G.; Moffat, H.K.; Schoegl, I.; Speth, R.L.; Weber, B.W. *Cantera: An Object-Oriented Software Toolkit for Chemical Kinetics, Thermodynamics, and Transport Processes, Version 2.5.1*; Cantera Developers: Warrenville, IL, USA, 2017.

33. Methling, T.; Braun-Unkhoff, M.; Riedel, U. A novel linear transformation model for the analysis and optimisation of chemical kinetics. *Combust. Theory Model.* **2017**, *21*, 503–528. [CrossRef]

34. Shao, J.; Choudhary, R.; Peng, Y.; Davidson, D.F.; Hanson, R.K. A shock tube study of n-heptane, iso-octane, n-dodecane and iso-octane/n-dodecane blends oxidation at elevated pressures and intermediate temperatures. *Fuel* **2019**, *243*, 541–553. [CrossRef]

35. Johnson, M.S.; Pang, H.-W.; Liu, M.; Green, W.H. Species Selection for Automatic Chemical Kinetic Mechanism Generation. *ChemRxiv* **2024**. *preprint*. [CrossRef]

36. RMG-Py Github Repository, Issue Section, Issue Number 2521. Available online: https://github.com/ReactionMechanismGenerator/RMG-Py/issues/2521 (accessed on 18 December 2023).

37. Methling, T.; Braun-Unkhoff, M.; Riedel, U. An optimised chemical kinetic model for the combustion of fuel mixtures of syngas and natural gas. *Fuel* **2020**, *262*, 116611. [CrossRef]

38. Baulch, D.L.; Bowman, C.T.; Cobos, C.J.; Cox, R.A.; Just, T.; Kerr, J.A.; Pilling, M.J.; Stocker, D.; Troe, J.; Tsang, W.; et al. Evaluated Kinetic Data for Combustion Modeling: Supplement II. *J. Phys. Chem. Ref. Data* **2005**, *34*, 757–1397. [CrossRef]

39. Ranzi, E.; Frassoldati, A.; Stagni, A.; Pelucchi, M.; Cuoci, A.; Faravelli, T. Reduced Kinetic Schemes of Complex Reaction Systems: Fossil and Biomass-Derived Transportation Fuels. *Int. J. Chem. Kinet.* **2014**, *46*, 512–542. [CrossRef]
40. Mehl, M.; Pitz, W.J.; Westbrook, C.K.; Curran, H.J. Kinetic modeling of gasoline surrogate components and mixtures under engine conditions. *Proc. Combust. Inst.* **2011**, *33*, 193–200. [CrossRef]
41. Fieweger, K.; Blumenthal, R.; Adomeit, G. Self-ignition of S.I. engine model fuels: A shock tube investigation at high pressure. *Combust. Flame* **1997**, *109*, 599–619. [CrossRef]
42. AlAbbad, M.; Javed, T.; Khaled, F.; Badra, J.; Farooq, A. Ignition delay time measurements of primary reference fuel blends. *Combust. Flame* **2017**, *178*, 205–216. [CrossRef]
43. Herbinet, O.; Husson, B.; Serinyel, Z.; Cord, M.; Warth, V.; Fournet, R.; Glaude, P.-A.; Sirjean, B.; Battin-Leclerc, F.; Wang, Z.; et al. Experimental and modeling investigation of the low-temperature oxidation of n-heptane. *Combust. Flame* **2012**, *159*, 3455–3471. [CrossRef] [PubMed]